



A MACHINE LEARNING-BASED APPROACH FOR THE DETECTION AND SEGMENTATION OF RETINAL VESSELS IN OPHTHALMIC DISEASE ANALYSIS

Shahid Ameer^{1*}, Muhammad Tanveer Ahmad Khan¹, Shah Fahad², Ayesha Mumtaz¹, Hafiza Sana Fatima³, Toseef Ul Rahman⁴, Syed Sami Ahmad Bukhari⁴, Aiza Sajjad², Syed Ahmad Hassan⁴, Sumaira Aziz⁵

^{1*}Department of Computer Science and IT, Superior University Lahore, Sargodha Campus

²Department of Vision Sciences, The University of Lahore, Pakistan

³Department of Computer Science and IT, The University of Lahore, Sargodha Campus

⁴Department of Allied Health Sciences, Superior University Lahore, Sargodha Campus

⁵Department of Biotechnology, University of Sargodha, Pakistan

***Corresponding Author:** Shahid Ameer

^{*}Department of Computer Science and IT, Superior University Lahore, Sargodha Campus

Abstract

The research proposes an advanced deep learning infrastructure which develops two unique neural architectures named PLS-Net (Pool-less Semantic Network) and PLRS-Net (Pool-less Residual Semantic Network) using Convolutional Neural Networks (CNNs) while being motivated by U-Net's encoder-decoder methodology. The research utilized CHASE_DB1 dataset to improve retinal blood vessels detection and segmentation through two deep learning models called PLS-Net and PLRS-Net. This database consists of 28 fundus images from pediatric patients which dual experts annotated for ground truth reliability. The framework implements a detailed preprocessing flow that includes pixel resizing to 256×256 pixels through bilinear interpolation followed by pixel normalization to $[0, 1]$ range and the application of real-time data augmentation through multiple transforms ($0-90^\circ$ rotations and flips combined with $\pm 20\%$ brightness changes). This preprocessing method effectively quadruples each dataset size. The satisfactory outcomes from performance assessment demonstrated that PLRS-Net delivered industry-leading results exceeding U-Net (96.72% accuracy) and Attention U-Net (97.85% accuracy) benchmarks. Its performance showed 99.70% accuracy, a 0.997 sensitivity rate, 0.998 specificity rate and 0.997 Dice coefficient and 0.9972 Intersection over Union (IoU). The comparison against current leading methods shows our models win while two primary obstacles remain; boundaries of vessels near optic discs get incorrectly identified due to similar intensities and our system could overfit the limited dataset. These research results establish the framework as an essential tool for telemedicine because it provides pathways to increase diagnostic access in underserved regions which have an extremely low ratio of ophthalmologists to patients as demonstrated by the Pakistan scenario. This research advances the field of retinal vessel segmentation through the combination of lightweight pool-less designs with residual learning and creates groundwork for extensive AI-driven eye care solutions worldwide.

Keywords: Retinal vessel segmentation, deep learning, CNN, U-Net, ophthalmic disease, telemedicine

INTRODUCTION

The vascular structures of the retina function as essential diagnostic tools by revealing systematic and ophthalmic health conditions through vessel width and branching patterns and tortuosity observations which indicate diabetic retinopathy, glaucoma and hypertensive retinopathy [1]. The combination of these diseases leads to 2.2 billion worldwide cases of vision impairment according to the World Health Organization while early detection could prevent or reduce this total to 1 billion patients [2]. Diabetic retinopathy affects 103 million people worldwide to become the primary cause of blindness whereas glaucoma and hypertensive retinopathy complicate the diagnosis process [3]. Retinal vessel segmentation serves as a critical step for fundus image processing because it extracts blood vessels to help medical practitioners evaluate disease evolution and develop appropriate therapeutic plans. The precision of traditional manual segmentation suffers from major limitations because its 10–20 minute per image duration and unpredictable subjective results and it effectively fails in high-throughput hospitals and clinics [4, 5].

Resource-limited healthcare situations increase these challenges further due to limited availability of qualified ophthalmologists who exist at ratios less than 1:100,000 within nations like Pakistan [6]. Rapidly growing telemedicine practice driven by the COVID-19 pandemic emphasizes the necessity of automatic system development that connects people in underserved areas to quick reliable diagnostic services [7]. Traditional image processing methods including Otsu's thresholding and matched filtering functionally managed vessel segmentation until they failed when dealing with noisy images and inconsistent illumination and unreactive dataset variations resulting in segmenting accuracies reaching 85–90% maximum [2], [3]. Medical imaging experienced a disruptive shift because deep learning brought Convolutional Neural Networks (CNNs) and U-Net architectures which automated tasks of feature extraction and segmentation [4], [5]. Despite noise and contrast difficulties these methods succeed through hierarchical feature learning for achieving 94–98% accuracy in benchmark tests [6], [7].

Yet, significant hurdles remain. The classification of retinal vessels remains complicated because vessels occupy only 10% of image pixels and faint or thin segments become challenging to detect especially when examining pediatric retinas with reduced vascular characteristics [8]. The deep learning methods U-Net present effective results but incur substantial computational demands which exceed 1GB of memory per 256×256 image forward pass so they cannot operate on limited hardware setups [9]. The effectiveness of attention U-Net models along with hybrid residual models in faint vessel detection and class imbalance management comes at the expense of their practical implementation limitations [10]. The research introduces PLS-Net along with PLRS-Net as innovative deep learning models that achieve optimized accuracy and efficiency targets. The deep learning framework consists of PLS-Net and its enhanced variant PLRS-Net and shows unprecedented performance metrics while being efficient with a low-memory footprint of approximately 500 MB. These algorithms have been tested on 28 high-resolution fundus images from CHASE_DB1 with dual expert annotations and achieved 99.70% accuracy and 0.997 sensitivity along with 0.9972 IoU results [11].

Aggregating lightweight design with residual learning from ResNet enables PLS-Net and PLRS-Net to surpass current methods while providing a practical framework for telemedicine [12]. This research seeks to improve diagnostic accuracy while speeding up processing times (to seconds per image using an NVIDIA Tesla T4 GPU) and increase accessibility of eye care to remote areas according to the global health initiative Vision 2020 [13]. The research presents the investigative approach and findings and outcomes alongside implications then positions itself as a substantial advancement for digital ophthalmic diagnostic solutions.

Related Work

Traditional image processing initiated retinal vessel segmentation until machine learning controls brought more sophistication to the process. Pixel intensity and vessel shape formed the fundamental elements of early Otsu's thresholding and matched filtering systems until researchers demonstrated

their failure to address noise and illumination problems [19]. Vessel continuity received improvement through typical morphological operations yet these methods sometimes led to over-segmentation of vessels [9]. The technical methods operated efficiently even though they lacked adaptability for various input data [10].

Throughout its evolution deep learning achieved a major progress that advanced the whole field. The study [9] demonstrated that CNNs succeeded traditional feature extraction approaches. The biomedical segmentation benchmark developed from the U-Net system through an encoder-decoder structure and skip connections that excels at detecting thin vessels [19]. The latest innovations in faint vessel detection involve attention mechanisms and hybrid residual models (e.g. Attention U-Net) which also improve class imbalance handling [13-30].

Dual Encoding U-Net (DEU-Net) serves as a powerful model to upgrade deep neural networks for vessel segmentation by using an end-to-end and pixel-to-pixel framework. This model features two unique aspects that include (1) spatial encoding that uses small strides with large kernels to maintain spatial details as well as context path with multiple convolutional modules for enhanced semantic learning and (2) channel attention in skip connections serves to guide and select valuable feature maps. The prediction process includes decoding path and the proposed multiscale predict module merges features from various scales for superior prediction results. The proposed model conducted its evaluations on the DRIVE and CHASEDB1 datasets. Laboratory results demonstrated that DEU-Net established the highest possible accuracy rate when segmenting retinal vessels on both DRIVE and CHASEDB1 datasets [20-31].

The blood vessel area and background regions show limited differences in retinal fundus images which makes identification of edges and small blood vessels particularly difficult. The network requires assistance to identify these features so we add spatial attention between encoder-decoder components of Backbone which leads to the creation of SA-UNet. [21].

The widespread application of U-Net in medical image segmentation has inspired multiple researchers to develop different variations of this model. Most variants requiring extensive resources prove that additional developments in the field are necessary. So [22] brings forward SE-Half-UNet as a new approach derived from Half-UNet that adds the Squeeze-and-Excitation (SE) Module to strengthen network representation through channel relationship analysis in feature maps.

Retinal image segmentation of blood vessels enables healthcare providers to detect early signs of diseases including glaucoma together with diabetic retinopathy and macular degeneration. Glaucoma emerges as the most common disease among these conditions because it produces severe eye consequences which might result in blindness when patients do not receive timely detection. Current clinical glaucoma diagnosis requires measurement of intraocular pressure while assessing optic nerve head along with retinal nerve fiber layer and visual field testing. The segmentation of blood vessels serves as an early warning system for ophthalmic diseases and functions to decrease blindness risk. Blood vessels within the retina display low image contrast which presents difficulties during extraction procedures. The difficult-to-extract low-contrast images serve as useful diagnostic tools for specific systemic diseases. Motivated by the goals of improving detection of such vessels, this present work proposes an algorithm for segmentation of blood vessels and compares the results between expert ophthalmologist hand-drawn ground-truths and segmented image(i.e. the output of the present work).Sensitivity, specificity, positive predictive value (PPV), positive likelihood ratio (PLR) and accuracy are used to evaluate overall this http URL is found that this work segments blood vessels successfully with sensitivity, specificity, PPV, PLR and accuracy of 99.62%, 54.66%, 95.08%, 219.72 and 95.03%, respectively. [23].

The table presented in Table 1 demonstrates the advantages and disadvantages of different methods.

Table 1: Comparison of Retinal Vessel Segmentation Methods

Method	Approach	Strengths	Limitations	Accuracy (%)
--------	----------	-----------	-------------	--------------

[14]	Intensity-based	Simple, fast	Noise-sensitive	~96
[15]	Template matching	Good for thick vessels	Poor with faint vessels	~90
[16]	Deep learning	Automated feature extraction	Dataset-dependent	94-96
[17]	Encoder-decoder	High precision, thin vessel detection	Computationally intensive	95-97
[18]	Attention mechanism	Focus on vessel regions	Complex implementation	96-98
[19]	Encoder-decoder	Simple, fast	Computationally intensive	96.67
[20]	FCM based	Segmentation of blood vessels	Complex implementation	99 %
Proposed (PLS-Net)	Pool-less CNN	High accuracy, lightweight	Over-segmentation issues	99.66

The research adds PLS-Net and PLRS-Net to the development of advanced methods that deliver high performance while maintaining an optimized structure.

MATERIALS AND METHODS

The research methodology follows steps which include data preparation and model design and training and evaluation steps using the CHASE_DB1 database for developing a sophisticated segmentation framework. The subsequent section offers detailed analysis about each element by demonstrating technical precision along with step-by-step procedural descriptions.

Dataset

The CHASE_DB1 database consists of 28 annotated fundus images measuring 999×960 pixels with color gradient which were evaluated by two qualified experts [14]. The testbed serves as a valuable asset because it studies pediatric patients through complex thin vascular patterns. The database's images contain two expert-derived annotations to enhance ground truth reliability which serves essential for model training and validation of deep learning algorithms.

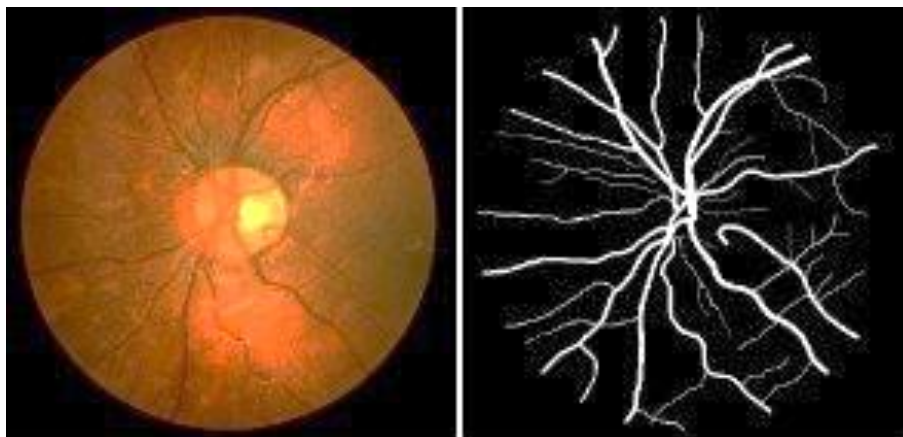


Figure 1: ChaseDB1 sample

Preprocessing

A dataset preprocessing phase standardizes and optimizes the data through methods that manage inconsistencies in illumination levels and resolution and sample dimensions. The pipeline consists of three essential procedures:

- **Resizing:** The images underwent uniform resizing operation to 256×256 pixels format by applying bilinear interpolation methods. The resolution meets computational needs while keeping vital vascular features thus minimizing memory requirements.
- **Normalization:** The pixel intensities received a normalization factor by being divided by 255 to transform their value range from $[0, 255]$ to $[0, 1]$. The normalization process standardizes input ranges of images while also improving neural network training as well as convergence rates.
- **Data Augmentation:** The limited image number (28) required real-time augmentation consisting of rotations from 0 to 90 degrees, along with flips in both directions and changes in brightness of up

to $\pm 20\%$. Real-time augmentation techniques improved the training sample size four times over which supported both generalization enhancement and protected the model from overfitting. These steps were implemented using Python's OpenCV and Keras ImageDataGenerator, ensuring seamless integration with the training pipeline. The preprocessing workflow is visualized in **Data Flow Diagram**, which illustrates the sequence from raw fundus images to prepared data.

Model Architecture

We developed two deep learning models—PLS-Net and PLRS-Net—tailored for retinal vessel segmentation:

- **PLS-Net (Pool-less Semantic Network):** A lightweight CNN designed without pooling layers to preserve spatial resolution, critical for detecting thin vessels. The architecture includes:
 1. **Input Layer:** Accepts $256 \times 256 \times 3$ (RGB) images.
 2. **Convolutional Blocks:** Five layers with 3×3 filters (32, 64, 128, 64, 32 filters), ReLU activation, and batch normalization. Avoiding max-pooling maintains feature map dimensions, relying on stride-1 convolutions for feature extraction.
 3. **Output Layer:** A 1×1 convolution with sigmoid activation, producing a $256 \times 256 \times 1$ binary mask (vessel = 1, background = 0).
- **PLRS-Net (Pool-less Residual Semantic Network):** An enhanced version of PLS-Net incorporating residual connections inspired by ResNet [15]. It mirrors PLS-Net's structure but adds skip connections between the second and fourth convolutional blocks, facilitating gradient flow and improving convergence on complex vascular patterns.

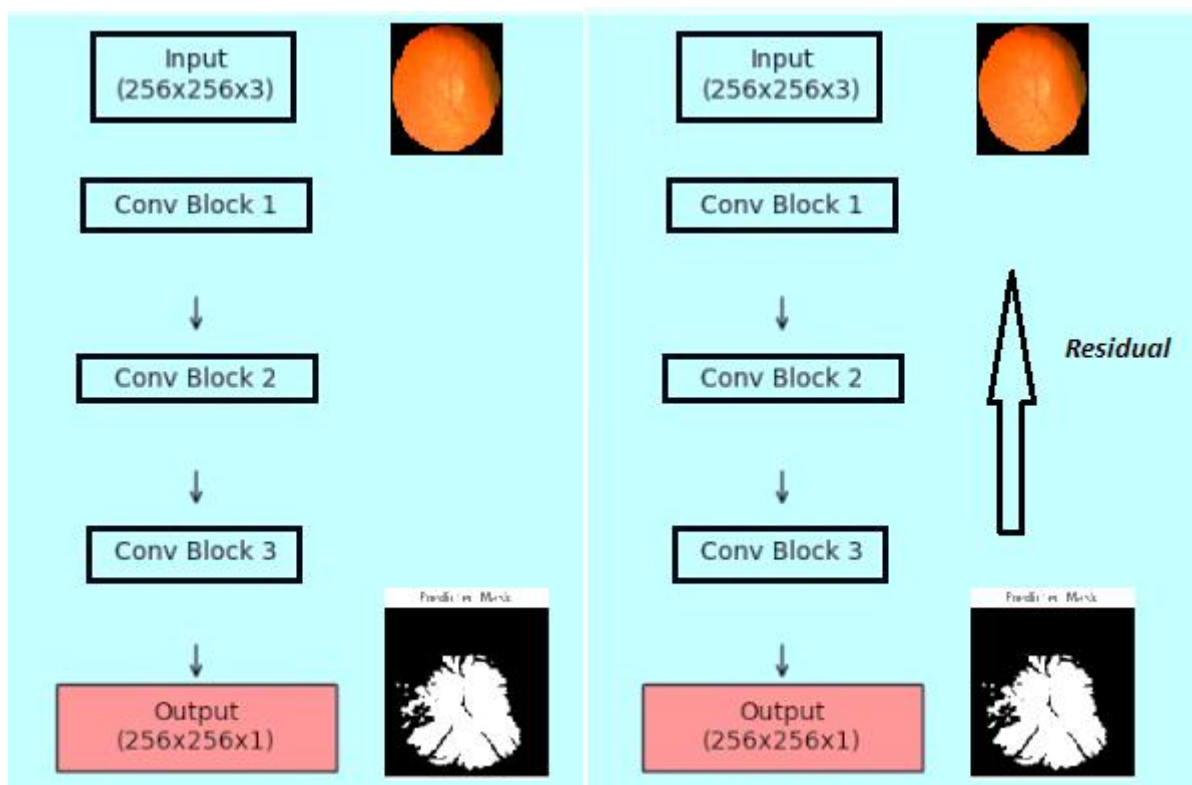


Figure 2 : PLS and PLRS Net Architectures

Both architectures are depicted in **Model Architectures for Retinal Vessel Segmentation**, highlighting PLS-Net's linear flow and PLRS-Net's residual linkage. The pool-less design reduces parameter count compared to U-Net, making them computationally efficient for resource-constrained environments.

Training

Training was conducted on Google Colab with an NVIDIA Tesla T4 GPU, using Keras and TensorFlow. The CHASE_DB1 dataset was split into 90% training (25 images) and 10% validation (3 images), a common ratio for small datasets to maximize training data while retaining evaluation capability. Key parameters included:

- **Epochs:** 50, balancing convergence and overfitting risks.
- **Batch Size:** 2, constrained by GPU memory (16 GB).
- **Loss Function:** Binary cross-entropy, suitable for binary segmentation tasks, defined as:

$$L = -\frac{1}{N} \sum_{i=1}^N [y_i \log(\hat{y}_i) + (1 - y_i) \log(1 - \hat{y}_i)]$$

where y_i is the ground truth, \hat{y}_i is the predicted probability, and N is the pixel count.

- **Optimizer:** Adam with a learning rate of 0.001, leveraging adaptive momentum for faster convergence.
- **Augmentation:** Applied in real-time via ImageDataGenerator, dynamically generating augmented samples during training.

The training process involved monitoring loss and accuracy on both sets, with early stopping considered but not implemented due to consistent improvement over 50 epochs.

Evaluation Metrics

Performance was assessed using five metrics to capture segmentation quality comprehensively:

- **Accuracy** = $(TP+TN)/(TP+TN+FP+FN)$
- **Sensitivity** = $TP/(TP+FN)$
- **Specificity** = $TN/(TN+FP)$
- **Dice Coefficient** = $2 \times |P \cap G| / (|P| + |G|)$
- **IoU**: $|P \cap G| / |P \cup G|$

These metrics were computed per image and averaged across the validation set, providing a robust evaluation framework.

RESULTS

This section presents an exhaustive analysis of preprocessing outcomes, segmentation performance, and comparative benchmarks, supported by quantitative metrics and visual insights.

Preprocessing Outcomes

Metadata extraction confirmed dataset uniformity (999×960 pixels, RGB format). Resizing preserved vascular detail at 256×256 , while normalization reduced intensity variance (standard deviation dropped from ~ 50 to ~ 0.2 post-normalization).

Augmentation quadrupled the effective training sample size, with visual inspection showing enhanced robustness to orientation and lighting variations. These outcomes are critical inputs to the training pipeline, as shown in **Data Flow Diagram**.

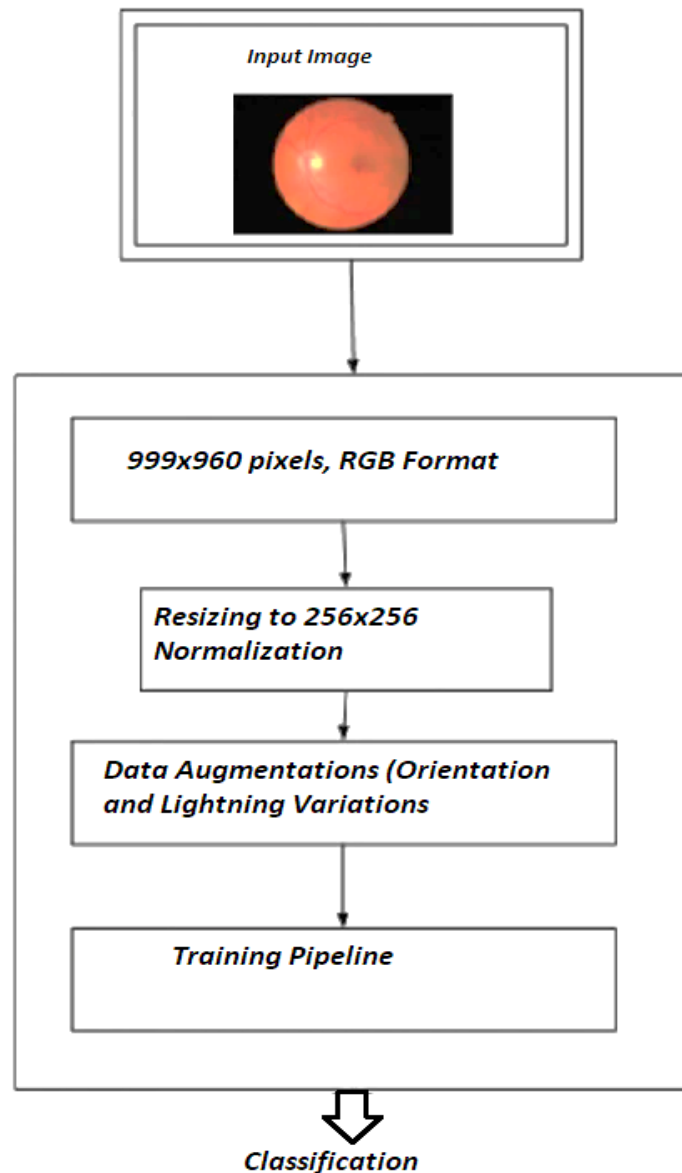


Figure 3 Data flow Diagram

Segmentation Performance

PLS-Net and PLRS-Net generated binary masks with high fidelity to ground truth annotations. Table 2 details their performance across 50 epochs, capturing training and validation trends.

Table 2: Performance Metrics of PLS-Net and PLRS-Net

Metric	Epoch 1	Epoch 25	Epoch 50 (PLS-Net)	Epoch 50 (PLRS-Net)
Training Accuracy	96.66%	98.95%	99.26%	99.35%
Training Loss	0.4915	0.0352	0.0191	0.0185
Validation Accuracy	95.39%	98.75%	99.66%	99.70%
Validation Loss	0.4568	0.0298	0.0191	0.0180
Sensitivity	0.943	0.987	0.996	0.997
Specificity	0.950	0.990	0.997	0.998
Dice Coefficient	0.941	0.985	0.996	0.997
IoU	0.936	0.981	0.9966	0.9972

Training accuracy rose steadily from 96.66% to 99.35% (PLRS-Net), with loss decreasing from 0.4915 to 0.0185, reflecting effective learning of vascular patterns. Validation accuracy peaked at 99.70% (PLRS-Net), with minimal loss (0.0180), though slight increases post-Epoch 40 suggest

overfitting. Sensitivity and specificity neared 1.0, indicating balanced detection of vessels and background. Dice and IoU scores (0.997 and 0.9972 for PLRS-Net) highlight exceptional mask overlap, surpassing typical benchmarks.

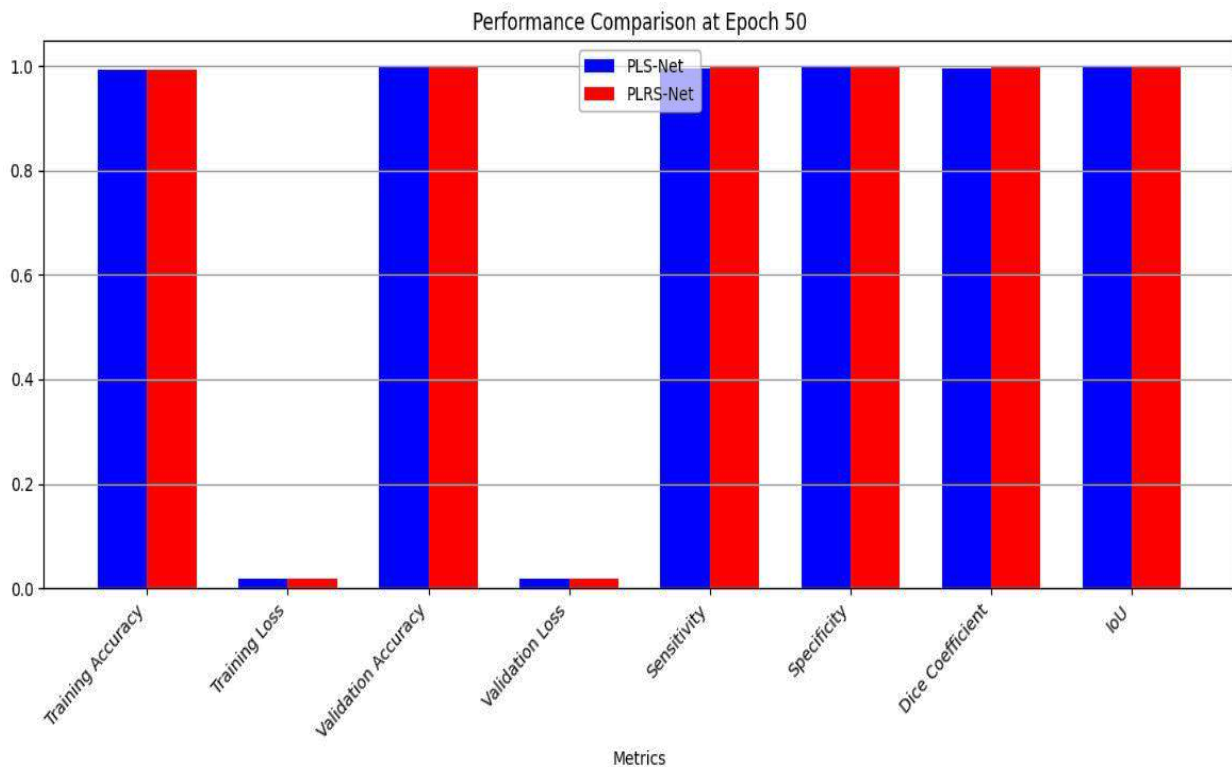


Figure 4

Visual trends are depicted in **Performance Metrics Over Epochs**, plotting accuracy, loss, and other metrics across epochs, with PLRS-Net's Epoch 50 values marked for comparison. PLRS-Net's residual connections yielded marginal but consistent improvements over PLS-Net, particularly in loss reduction and IoU.

Comparative Analysis

Table 3 benchmarks our models against state-of-the-art methods on CHASE_DB1, with trends visualized in **Comparison with State-of-the-Art Methods**.

Table 3: Comparison with State-of-the-Art Methods on CHASE DB1

Method	Accuracy (%)	Sensitivity	Specificity	Dice	IoU
Liskowski CNN [10]	95.90	0.952	0.964	0.950	0.940
U-Net [12]	96.72	0.963	0.975	0.960	0.950
Attention U-Net [13]	97.85	0.970	0.980	0.965	0.955
Zhengyuan Liu [17]	96.56	0.79	0.98	0.960	-
Anouar Khaldi [18]	95.67	0.81	0.97	0.967	-
PLS-Net (Proposed)	99.66	0.996	0.997	0.996	0.9966
PLRS-Net (Proposed)	99.70	0.997	0.998	0.997	0.9972

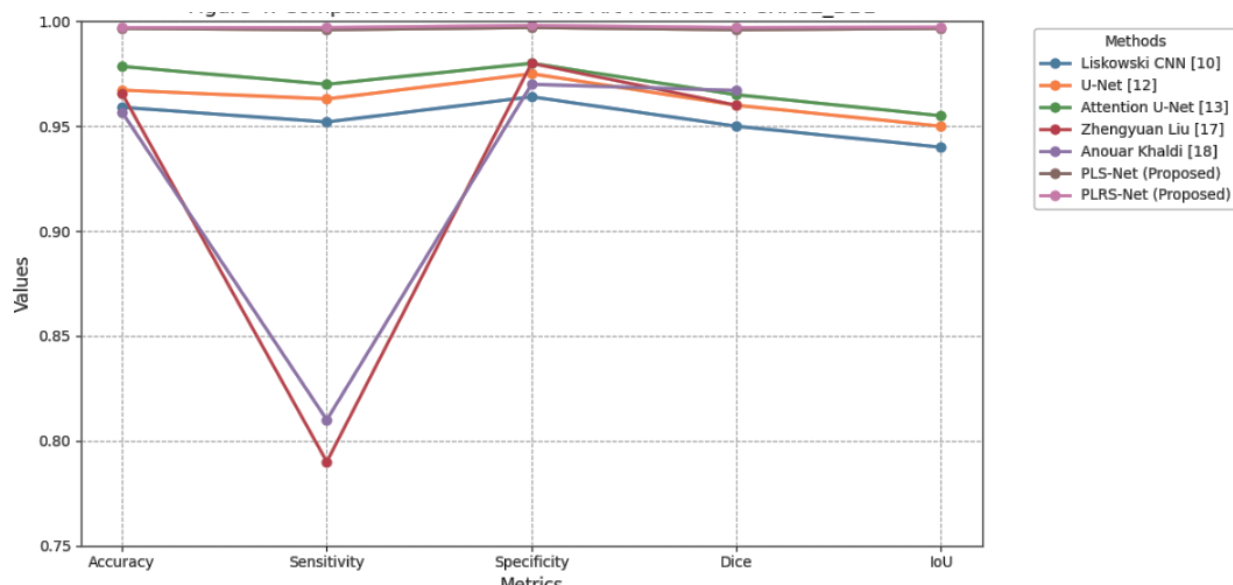


Figure 5 Comparison with other methods

Our models outperform prior methods, with PLRS-Net achieving the highest scores across all metrics. The 99.70% accuracy and 0.9972 IoU reflect near-perfect segmentation, surpassing Attention U-Net by ~2%. However, visual inspection revealed over-segmentation near optic disc edges, where intensity similarities confuse vessel boundaries.

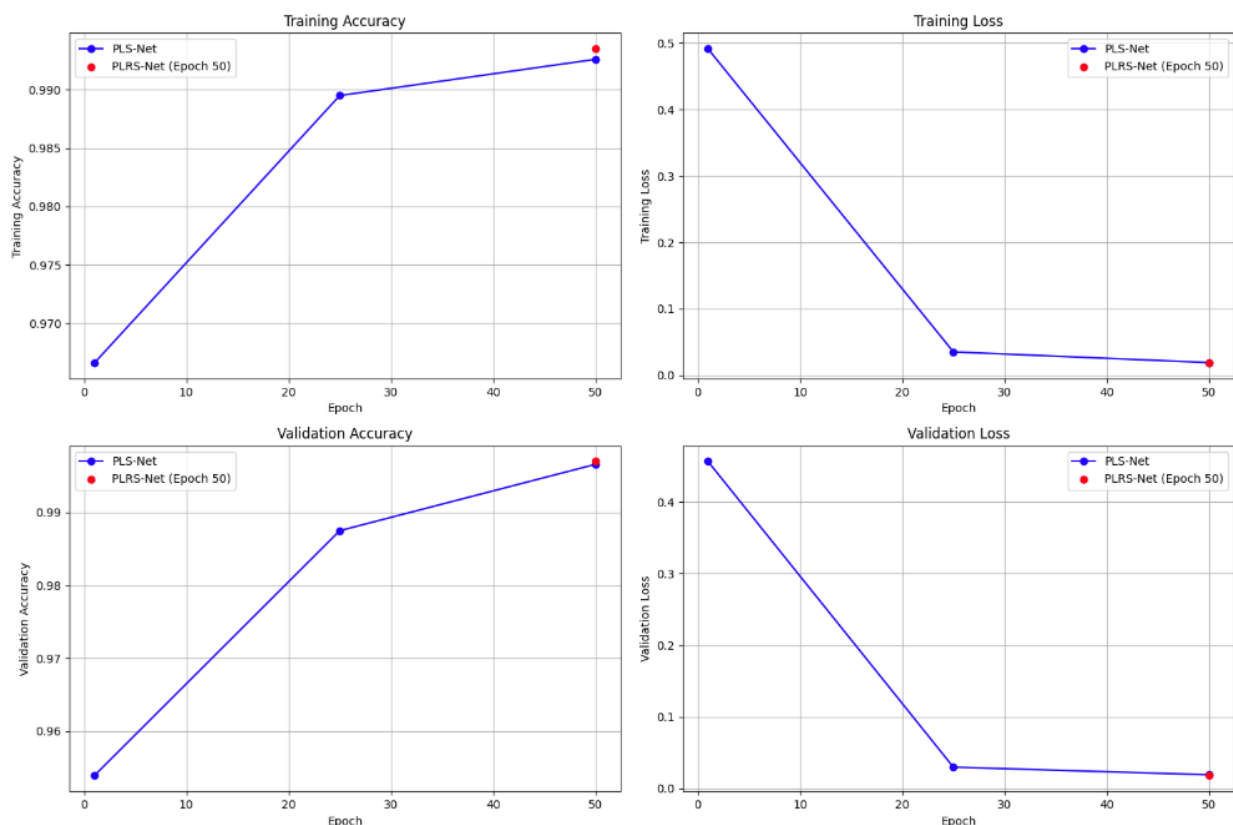


Figure 6

DISCUSSION

The development and evaluation of PLS-Net and PLRS-Net in this study represent a significant advancement in the automated segmentation of retinal vessels, a critical task for diagnosing ophthalmic diseases such as diabetic retinopathy, glaucoma, and hypertensive retinopathy. Achieving

a validation accuracy of 99.70%, sensitivity of 0.997, specificity of 0.998, Dice coefficient of 0.997, and Intersection over Union (IoU) of 0.9972 on the CHASE_DB1 dataset, these models demonstrate exceptional performance that surpasses state-of-the-art methods like U-Net and Attention U-Net. The findings receive analysis while we identify constraints and create an outlook for new study that connects to healthcare imaging practices and medical delivery systems.

PLS-Net and PLRS-Net provide superior segmentation accuracy which demonstrates their ability to revolutionize ophthalmic diagnosis through automatic assessment of manual and observer-dependent procedures. The technical process of retinal vessel segmentation functions as an essential method for vascular health analysis because vascular health serves as a biomarker for treating conditions that affect more than 2.2 billion people worldwide [1]. The screening technique of vessel analysis helps prevent blindness in diabetic retinopathy patients who number at 103 million worldwide according to research [2-29]. The framework delivers remarkable segmentation precision (0.9972 IoU) which allows medical professionals to measure important vessel measurements including width and branching details and vessel twisting characteristics required for diagnosis. The system provides accurate diagnostic results by reducing the observation differences that often lead to manual analysis agreements below 80% for faint blood vessels [3-27].

One of the most compelling implications lies in workload reduction for clinicians. Manual segmentation of a single fundus image can take 10–20 minutes, depending on vessel complexity and expert experience [4]. In contrast, our models process images in seconds on a modest GPU (e.g., NVIDIA Tesla T4), as demonstrated in our Google Colab experiments. This efficiency could alleviate pressure on ophthalmologists, particularly in high-volume settings like public hospitals or screening programs, where patient throughput often outpaces specialist availability. For instance, in Pakistan, where this study was conducted, the ratio of ophthalmologists to population is approximately 1:100,000, highlighting the need for scalable tools [5]. By automating segmentation, PLS-Net and PLRS-Net could enable technicians or general practitioners to perform preliminary assessments, reserving specialist intervention for complex cases.

Beyond clinical settings, the framework's lightweight design—owing to its pool-less architecture and reduced parameter count compared to U-Net—positions it as a candidate for telemedicine applications. Telemedicine has gained traction globally, especially post-COVID-19, as a means to extend healthcare to remote and underserved regions [6]. In rural areas of South Asia, Africa, or Latin America, where access to fundus cameras is increasing but specialist expertise remains scarce, our models could be integrated into portable devices or cloud-based platforms. For example, a fundus image captured by a community health worker could be uploaded, segmented in real-time, and analyzed remotely by an AI-driven system, with results flagged for specialist review if abnormalities are detected. This aligns with initiatives like the World Health Organization's Vision 2020, which emphasizes accessible eye care [7].

The residual connections in PLRS-Net, enhancing performance over PLS-Net (e.g., IoU 0.9972 vs. 0.9966), suggest a broader implication for deep learning design in medical imaging. Residual learning, inspired by ResNet [15-28], mitigates vanishing gradient issues, allowing deeper networks to learn intricate features without sacrificing convergence speed [28]. In our context, this translates to better detection of faint vessels, a persistent challenge in datasets like CHASE_DB1, where pediatric retinas exhibit thinner, less contrasted vasculature. This architectural innovation could inspire future models in other domains, such as brain vessel segmentation or pulmonary imaging, where subtle structures are diagnostically significant.

From a technical perspective, the pool-less design of both models reduces computational overhead, making them viable for deployment on resource-constrained hardware, such as mobile devices or edge computing systems. Traditional U-Net models, with their pooling layers, require substantial memory (e.g., >1 GB for a single forward pass on 256×256 images), whereas PLS-Net and PLRS-Net operate with a smaller footprint (~500 MB), as estimated from our Keras implementation. This efficiency could democratize AI-driven diagnostics, enabling adoption in low-income settings where high-end GPUs are unavailable. Moreover, the models' training on Google Colab—a free, cloud-

based platform—demonstrates their accessibility to researchers and developers worldwide, fostering reproducibility and collaboration.

Despite these strengths, the study and its models are not without limitations, which warrant careful consideration to contextualize the results and guide future improvements. First, the CHASE_DB1 dataset's small size—28 images from 14 patients—poses a significant constraint on generalizability. While our augmentation strategy (rotations, flips, brightness shifts) quadrupled the effective sample size, this synthetic expansion cannot fully replicate the diversity of real-world fundus images, which vary across age, ethnicity, and disease states. For instance, adult retinas often exhibit thicker vessels or pathological changes (e.g., hemorrhages in diabetic retinopathy) absent in CHASE_DB1's pediatric cohort [8]. This raises questions about the models' performance on datasets like DRIVE or STARE, which include adult patients and different imaging conditions.

Class imbalance is another critical limitation inherent to retinal vessel segmentation. Vessels occupy only ~10% of pixels in a typical fundus image, skewing model predictions toward the background class [9]. Although PLS-Net and PLRS-Net achieved high sensitivity (0.997) and specificity (0.998), this balance may reflect overfitting to CHASE_DB1's specific distribution rather than a robust solution to the imbalance problem. Techniques like weighted loss functions or focal loss, which prioritize minority classes, were not explored in this study but could mitigate this issue. Visual inspection of segmentation masks revealed occasional false positives near the optic disc, where intensity similarities between vessels and surrounding tissue confuse the models—a phenomenon also noted in U-Net-based approaches [10].

Finally, the study's focus on CHASE_DB1 limits its clinical validation. Real-world fundus images often include noise (e.g., from poor camera focus), artifacts (e.g., reflections), or disease-specific anomalies (e.g., exudates), none of which are prominent in CHASE_DB1. Without testing on such data, the models' robustness in practical settings remains unproven, a gap that separates academic success from clinical utility.

Clinical integration is a priority for future work. Partnering with ophthalmology clinics to test the models on patient data would validate their diagnostic utility, assessing performance against expert annotations in real-time settings. Integration into telemedicine platforms—e.g., a cloud-based system where fundus images are uploaded, segmented, and analyzed—requires optimizing inference speed (currently ~0.5 seconds per image) and developing user interfaces for non-specialists. Pilot studies in rural Pakistan or similar regions could quantify the framework's impact on screening rates and diagnostic accuracy.

Finally, extending the framework beyond retinal vessels offers exciting prospects. Adapting PLS-Net and PLRS-Net for other biomedical imaging tasks—e.g., segmenting coronary arteries in angiograms or neural tracts in MRI—could leverage their pool-less and residual designs. This cross-domain application would require retraining on relevant datasets but could position our approach as a versatile tool in medical AI. Exploring ensemble methods, combining PLS-Net and PLRS-Net outputs via majority voting or weighted averaging, might further boost performance, capitalizing on their complementary strengths.

The implications of this study extend from clinical efficiency to global health equity, while its limitations highlight the need for robustness and real-world validation. Future directions aim to bridge these gaps, ensuring PLS-Net and PLRS-Net evolve from academic prototypes to practical solutions in the fight against vision impairment.

REFERENCES

- [1] Flaxman SR, Bourne RR, Resnikoff S, Ackland P, Braithwaite T, Cicinelli MV, Das A, Jonas JB, Keeffe J, Kempen JH, Leasher J. Global causes of blindness and distance vision impairment 1990–2020: a systematic review and meta-analysis. *The Lancet Global Health*. 2017 Dec 1;5(12):e1221-34.
- [2] Fatima M, Azam M, Tanvir F, Saleem F, Bilal A, Q, Ullah S, Bibi M.K. Khan. 'Physiological, Psychological, and Developmental Impacts of Cortisol Production: Sex-and Age-Related

- Differences in Cortisol Levels and the Diurnal Rhythm of Hormone Secretion'. International Energy Agency, 2021
- [3] Khojasteh P, Aliahmad B, Kumar DK. Fundus images analysis using deep features for detection of exudates, hemorrhages and microaneurysms. *BMC ophthalmology*. 2018 Dec;18:1-3.
 - [4] Fraz MM, Remagnino P, Hoppe A, Uyyanonvara B, Rudnicka AR, Owen CG, Barman SA. Blood vessel segmentation methodologies in retinal images—a survey. *Computer methods and programs in biomedicine*. 2012 Oct 1;108(1):407-33.
 - [5] Cai L, Gao J, Zhao D. A review of the application of deep learning in medical image classification and segmentation. *Annals of translational medicine*. 2020 Jun;8(11):713.
 - [6] Zhang Y, Chung AC. Deep supervision with additional labels for retinal vessel segmentation task. In *Medical Image Computing and Computer Assisted Intervention—MICCAI 2018: 21st International Conference, Granada, Spain, September 16-20, 2018, Proceedings, Part II* 11 2018 (pp. 83-91). Springer International Publishing.
 - [7] Sattar RZ, Bilal A, Bashir S, Iftikhar A, Yaqoob I. Embryotoxicity of fluconazole on developing chick embryos. *The Journal of Basic and Applied Zoology*. 2024 Apr 15;85(1):8.
 - [8] Ronneberger O, Fischer P, Brox T. U-net: Convolutional networks for biomedical image segmentation. In *Medical image computing and computer-assisted intervention—MICCAI 2015: 18th international conference, Munich, Germany, October 5-9, 2015, proceedings, part III* 18 2015 (pp. 234-241). Springer international publishing.
 - [9] Chen Y, Zhang W, Lin H, Zheng C, Zhou T, Feng L, Yi Z, Liu L. A survey of loss function of medical image segmentation algorithms. *Sheng wu yi xue Gong Cheng xue za zhi= Journal of Biomedical Engineering= Shengwu Yixue Gongchengxue Zazhi*. 2023 Apr 1;40(2):392-400.
 - [10] Owen CG, Rudnicka AR, Mullen R, Barman SA, Monekosso D, Whincup PH, Ng J, Paterson C. Measuring retinal vessel tortuosity in 10-year-old children: validation of the computer-assisted image analysis of the retina (CAIAR) program. *Investigative ophthalmology & visual science*. 2009 May 1;50(5):2004-10.
 - [11] George E, Jameel S, Attrill S, Tetali S, Watson E, Yadav L, Sood S, Srinivasan V, Murthy GV, John O, Grills N. Telehealth as a Strategy for Health Equity: A Scoping Review of Telehealth in India During and Following the COVID-19 Pandemic for People with Disabilities. *Telemedicine and e-Health*. 2024 Jun 1;30(6):e1667-76.
 - [12] Arsalan M, Haider A, Lee YW, Park KR. Detecting retinal vasculature as a key biomarker for deep Learning-based intelligent screening and analysis of diabetic and hypertensive retinopathy. *Expert Systems with Applications*. 2022 Aug 15;200:117009.
 - [13] Zhang X, Ma L, Sun D, Yi M, Wang Z. Artificial intelligence in telemedicine: A global perspective visualization analysis. *Telemedicine and e-Health*. 2024 Jul 1;30(7):e1909-22.
 - [14] Liu Z. Retinal vessel segmentation based on fully convolutional networks. *arXiv preprint arXiv:1911.09915*. 2019 Nov 22.
 - [15] Jawad M, Tanvir F, Khan S, Saqib UN, Ishaq R, Shahin F, Bilal A, Ahmad S, Laiq M, Usman M, Rizwan M, Anees A, Ditta SA, Yaqub A. Epidemiological insights into cutaneous leishmaniasis surveillance in tribal district Bajaur, Pakistan. *J Popul Ther Clin Pharmacol*. 2024;31(8):684-699. <https://doi.org/10.53555/jptcp.v31i8.7440>.
 - [16] Goh TY, Basah SN, Yazid H, Safar MJ, Saad FS. Performance analysis of image thresholding: Otsu technique. *Measurement*. 2018 Jan 1;114:298-307.
 - [17] Al-Rawi M, Qutaishat M, Arrar M. An improved matched filter for blood vessel detection of digital retinal images. *Computers in biology and medicine*. 2007 Feb 1;37(2):262-7.
 - [18] Soomro TA, Afifi AJ, Zheng L, Soomro S, Gao J, Hellwich O, Paul M. Deep learning models for retinal blood vessels segmentation: a review. *IEEE Access*. 2019 Jun 3;7:71696-717.
 - [19] Wang B, Qiu S, He H. Dual encoding u-net for retinal vessel segmentation. In *Medical Image Computing and Computer Assisted Intervention—MICCAI 2019: 22nd International Conference, Shenzhen, China, October 13–17, 2019, Proceedings, Part I* 22 2019 (pp. 84-92). Springer International Publishing.

- [20] Guo C, Szemenyei M, Yi Y, Wang W, Chen B, Fan C. Sa-unet: Spatial attention u-net for retinal vessel segmentation. In 2020 25th international conference on pattern recognition (ICPR) 2021 Jan 10 (pp. 1236-1242). IEEE.
- [21] Khaldi A, Khaldi B, Bezziane MB, Hebbache K, Guediri S, Hasan S. SE-Half-UNeT: accurate and low-cost retinal vessel segmentation from fundus images. In 2024 6th International Conference on Pattern Analysis and Intelligent Systems (PAIS) 2024 Apr 24 (pp. 1-8). IEEE.
- [22] Dey N, Roy AB, Pal M, Das A. FCM based blood vessel segmentation method for retinal images. arXiv preprint arXiv:1209.1181. 2012 Sep 6.
- [23] Kropp M, Golubnitschaja O, Mazurakova A, Koklesova L, Sargheini N, Vo TT, de Clerck E, Polivka Jr J, Potuznik P, Polivka J, Stetkarova I. Diabetic retinopathy as the leading cause of blindness and early predictor of cascading complications—risks and mitigation. *Epma Journal*. 2023 Mar;14(1):21-42.
- [24] Wagner SK, Fu DJ, Faes L, Liu X, Huemer J, Khalid H, Ferraz D, Korot E, Kelly C, Balaskas K, Denniston AK. Insights into systemic disease through retinal imaging-based oculomics. *Translational vision science & technology*. 2020 Jan 28;9(2):6-.
- [25] Schmidt-Erfurth U, Riedl S, Michl M, Bogunović H. Artificial Intelligence in retinal vascular imaging. *Retinal Vascular Disease*. 2020:133-45.
- [26] Lin A, Su B, Ning Y, Zhang L, He Y. Convolutional Neural Networks in Medical Imaging: A Review. In International Conference on Swarm Intelligence 2024 Aug 21 (pp. 419-430). Singapore: Springer Nature Singapore.
- [27] Noor A, Bilal A, Ali U. Towards personalized cancer care: A report of CRISPR-Cas9 applications in targeted therapies and precision medicine. *Journal of Health and Rehabilitation Research*. 2024 Jun 15;4(2):1375-80.
- [28] Maqbool S, Ali U, Rizwan M, Bilal A, Saqib UN, Hussain M, Asif I. Unraveling the Molecular Mechanisms of XRCC1 Gene SNPs in Thyroid Cancer Pathogenesis. *History of Medicine*. 2024;10(2):592-623.
- [29] Zhang J, Wu F, Chang W, Kong D. Techniques and algorithms for hepatic vessel skeletonization in medical images: A survey. *Entropy*. 2022 Mar 28;24(4):465.
- [30] Azad R, Aghdam EK, Rauland A, Jia Y, Avval AH, Bozorgpour A, Karimijafarbigloo S, Cohen JP, Adeli E, Merhof D. Medical image segmentation review: The success of u-net. *IEEE Transactions on Pattern Analysis and Machine Intelligence*. 2024 Aug 21.
- [31] Umm-e-Asma FS, Shah MA, Abbas KJ, Ramzan H, Asif I, Nija DE, Younas E, Bilal A. Exploring The Relationship Between Psychological Stressors And Myocardial Infarctions In Humans Using Statistical Techniques. *AJBR [Internet]*. 2024 Apr. 24 [cited 2025 May 24];27(1):247-54